JOURNAL OF MATERIALS SCIENCE 29 (1994) 5887–5891

Nanometer-scale chemical compatibility between nickel aluminide and MgO films

M. NATHAN*, C. R. ANDERSON, J. S. AHEARN
Martin Marietta Laboratories, 1450 South Rolling Road, Baltimore,MD 21227, USA

The stability of the NiAl/MgO interface at temperatures in the range 800–1000 °C was studied on layered thin films of MgO/(Ni + Al)/MgO, using electron diffraction in transmission electron microscopy, and X-ray photoelectron spectroscopy. NiAl was formed by rapid thermal annealing (RTA) of the films at 300 °C, without affecting the interface. RTA at 800 °C, for 5 min induced a limited interfacial reaction which formed a spinel phase and Ni_3Al, but left most of the NiAl and MgO layers intact. In the earliest reaction stages, aluminium diffuses out from, and oxygen diffuses into NiAl. After RTA at 1000 °C for 100 s, the NiAl layer disintegrates completely, while the magnesium apparently evaporates from the MgO. While the NiAl/MgO system is shown to be chemically incompatible on the nanoscale, comparison with other aluminide/reinforcement systems shows it to be one of the more stable ones.

1. Introduction

The main intermetallic matrix composite (IMC) system being currently evaluated for high-temperature applications (ca. 1000–1200 °C) is based on nickel aluminide. Any candidate reinforcement in the NiAl matrix has to fulfil two criteria: (1) chemical compatibility, and (2) close match in the coefficient of thermal expansion (CTE). A theoretical evaluation by Misra [1] indicates that of all chemically compatible reinforcements, only La_2O_3, MgO, cubic ZrO_2 and $CaZrO_3$ are closely matched in CTE with NiAl at 827 °C. The difference between the CTE of MgO ($15.2 \times 10^{-6} K^{-1}$) and that of NiAl ($\sim 16 \times 10^{-6} K^{-1}$) is about 5%. Interestingly, there are no reports in the literature on the NiAl–MgO composite system, possibly because it is expected to be unstable in dynamic environments, which are predicted to bring about the evaporation of magnesium [1]. In addition, thermodynamic predictions of bulk chemical compatibility often fail in the nanoscale of the interface [2, 3]. It appears, in fact, that a nanoscale reaction, i.e. nanoscale chemical "incompatibility", is essential for bonding and therefore mechanical strength, and that its occurrence is a rule, rather than an exception, in most of the systems deemed chemically compatible (i.e. non-reacting). Bulk studies and thermodynamic calculations are still valuable in determining gross incompatibilities, which lead to the destruction of the reinforcements. This work presents and discusses results on the nanocompatibility of the NiAl–MgO system. As a by-product of the experimental method, one can also evaluate the effect of a dynamic exposure environment.

2. Experimental procedure

As in previous studies [2, 3], our main specimen was a thin film consisting of multilayers of nickel and aluminium "sandwiched" between two 30 nm thick MgO layers, Fig. 1. Nickel and aluminium thicknesses are listed in Table I. Two other specimens, one of Al/Ni multilayers without MgO, and the other of a 50 nm thick MgO film, underwent the same treatments and served as "standards". The films were desposited by electron-beam evaporation in an ultrahigh vacuum system with a base pressure of 5×10^{-8} torr (1 torr = 133.322 Pa). Pressures during evaporation were in the low 10^{-7} torr range for nickel and aluminium, and in the 10^{-6} torr range for MgO. The deposition was done simultaneously on Formvar-coated transmission electron microscope (TEM) molybdenum grids and on an oxidized silicon wafer. After deposition, the films were annealed in a quartz halogen lamp system under flowing argon (99.999% purity). Details are given elsewhere [4].

The aluminide was formed by reacting the nickel and aluminium layers at a temperature low enough (300 °C) to prevent reaction with MgO. For the thicknesses given in Table I, the theoretical aluminide stoichiometry corresponds to 50% at. Al, i.e. NiAl. The nanocompatibility was determined by examining the phases present after 800 °C, 300 s, and 1000 °C, 100 s, annealings using selected-area diffraction (SAD) patterns in a Jeol 100CX scanning TEM at 100 kV, and by X-ray photoelectron spectroscopy (XPS) coupled with depth profiling. The SAD was carried out at a nominal magnification of $\times 50000$, with a 20 μm diffraction aperture defining the selected area. Interplanar SAD *d*-spacings were calculated using a known camera length, calibrated both internally, and periodically externally with a gold standard. All standard diffraction data were taken from JCPDS [5].

An SSI ESCA 101 Small-Spot system was used for

* *Permanent address*: Faculty of Engineering, Tel-Aviv University, Israel.

0022–2461 © *1994 Chapman & Hall*

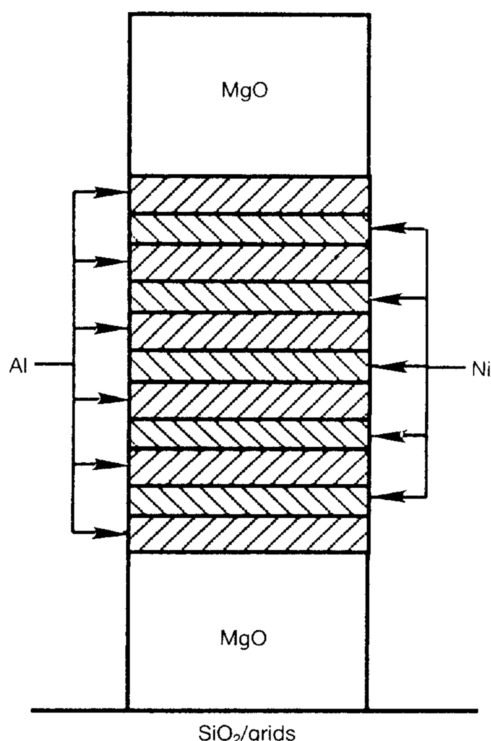

Figure 1 Schematic description of specimens used in study.

TABLE I Al/Ni layer thicknesses (nm). Top and bottom layers are 30 nm thick MgO

MgO	Al	Ni	Al	Ni	Al	Ni	Al	Ni	Al	Ni	Al	MgO
30	5	4	5	4	5	4	5	4	5	4	5	30

XPS. The system pressure was below 4×10^{-9} torr, prior to starting the argon leak into the ion-gun ionization chamber. A 600 μm X-ray spot was used in the depth profiles. The 4 keV argon ion beam was rastered over a diamond-shaped area with a long axis of about 4 mm and a short axis of about 3 mm. The calibrated sputter rate was 0.095 nm s^{-1} of SiO_2. The ion gun was a PHI Model 04-303 with a differential 50 l s^{-1} turbomolecular pump. A 56 l s^{-1} turbomolecular pump and a 240 l s^{-1} ion pump evacuated the analysis chamber during the depth profiles, keeping the pressure (mostly argon) in the $1\text{–}3 \times 10^{-7}$ torr range.

Because the sputter rate in XPS is a function of the material sputtered, the usual practice in a case like this is to use a timescale, while stating the calibrated sputter rate for a material such as SiO_2 or Ta_2O_5 under the same ion-gun operational conditions. Sometimes the calibrated rate is used to generate a depth scale, but this is somewhat fraudulent, because material sputter rates can differ by a factor of ten in extreme cases. We do not know the sputter rates for nickel aluminides nor NiO, and we only know approximately the sputter rates for MgO and Al_2O_3 relative to SiO_2. Therefore, the XPS depth profile is presented on a time (not depth) scale.

3. Results and discussion

3.1. Electron microscopy

Fig. 2 shows the SAD patterns of the as-deposited films. The MgO/Al/Ni film exhibits, as-expected, aluminium, nickel and MgO reflections. The standard Al/Ni specimen shows only aluminium and nickel reflections. In contrast with Al_2O_3 [2], room-temperature deposited MgO is crystalline and its pattern matches well the periclase (JCPDS 4-829) phase. Fig. 3 shows the patterns after rapid thermal annealing (RTA) at 300 °C for 100 s. The MgO/Al/Ni film consists now of very fine-grained (solid diffraction lines) aluminide. Using the internal MgO lines for calibration, the measured spacings of the additional solid lines (indicated by arrows) are 0.489, 0.348, 0.287, 0.201, 0.142 and 0.117 nm, which match very well Al_3Ni_2 (JCPDS 14-648). This a slightly more aluminium-rich phase than expected from the multilayer stoichiometry. Note that because the last four lines also match very well NiAl (JCPDS 2-1261 or 20-19), it is impossible to state unequivocally that the aluminide phase is not NiAl, and it may well be that both Al_3Ni_2 and NiAl coexist in the film. Nevertheless, because all lines are accounted for, it is clear that the aluminide forms at low temperature without a significant reaction between the individual layers (and particularly aluminium) and MgO. When the starting stoichiometry is changed to 55% Ni–45% Al, the 300 °C SAD pattern shows clearly only NiAl and MgO, and after subsequent annealings the results are identical to those in 50% Al films.

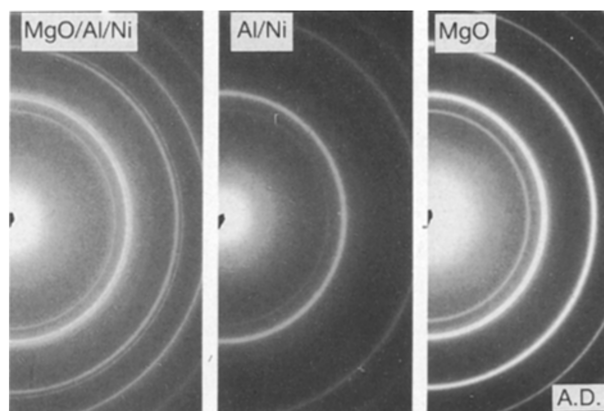

Figure 2 SAD patterns of as-deposited films.

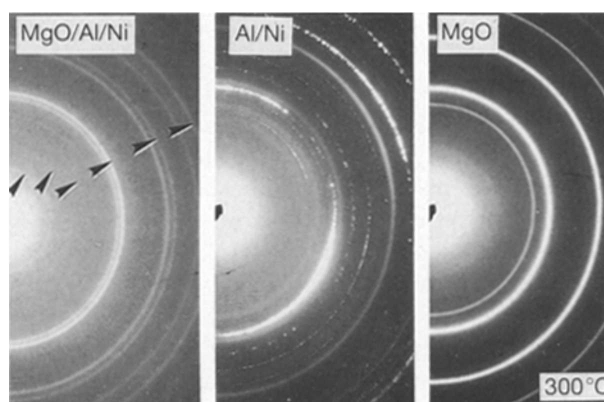

Figure 3 SAD patterns of films after annealing at 300 °C for 100 s.

The Al/Ni film shows Ni_3Al (JCPDS 9-97) and γ-Al_2O_3 (JCPDS 10-425) lines, while the MgO film is unchanged after the same RTA at 300 °C. Although having an overall Al/Ni ratio identical to MgO/Al/Ni, oxidation of its external aluminium layers, possibly by residual oxygen in the RTA chamber, deprives the film of enough aluminium so that Ni_3Al forms instead of Al_3Ni_2 or NiAl (a simple calculation [2] shows that without the 10 nm of the two external aluminium layers, the stack stoichiometry should be Ni_2Al). Formation of a metastable Al_2O_3 phase on NiAl in early oxidation stages is well established [6].

An additional RTA at 800 °C for 300 s yields the SAD patterns shown in Fig. 4, with their d-spacings listed in Table II. Through comparison with the two standard films and the 300 °C data, it is evident that a rather limited reaction took place. The arrows in the MgO/Al/Ni film point to the Al_3Ni_2 (NiAl) lines, still visible and quite strong. New dotted rings indicate the presence of a minor new phase. As shown in Table II, this phase is Ni_3Al. There is no evidence of Al_2O_3 being present. The presence of a weak line with $d = 0.468$ nm indicates that a minor amount of the spinel phase, $MgAl_2O_4$ (JCPDS 21-1152) has formed. Its presence at the interface between the aluminide and the top MgO layer is confirmed by XPS (see below). The standard Al/Ni film is practically unchanged from 300 °C. The standard MgO film shows an unidentified secondary phase, with lines which do not match any known magnesium oxide phase. Note (below) that this phase becomes dominant at 1000 °C. We conclude that the nickel aluminide/MgO system compares favourably with systems such as Al_2O_3/NiAl [7], and is more compatible at this temperature than other IMCs. Specifically, TiAl/MgO films annealed under identical conditions show no trace of TiAl, owing to its total consumption in the reaction [7].

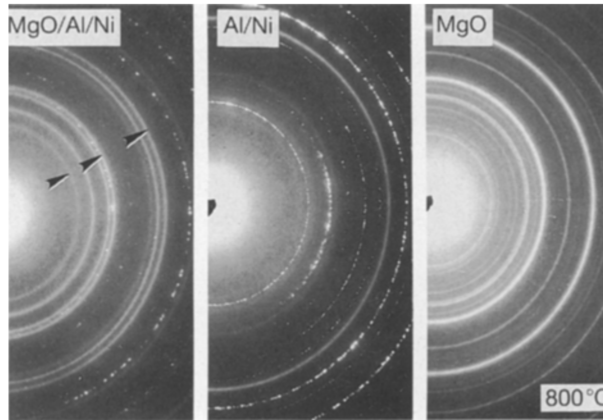

Figure 4 SAD patterns of films after additional annealing at 800 °C for 5 min.

TABLE II Interplanar spacings of films annealed at 3000 °C for 100 s + 800 °C for 300 s. s, strong; m, medium; w, weak; v, very,* Possible NiO reflections

Al/Ni	MgO	MgO/Al/Ni	Comments
Dotted rings	Solid rings	Solid rings	
2.54 m	5.12 vw	4.68 vvw	Spinel?
2.07 vs	3.92 m	3.94 vvw	MgO
1.78 vvw	3.75 vw	2.84 w	Al_3Ni_2 or NiAl
1.60 mw	3.49 w	2.44 s	MgO
1.47 mw*	3.01 m	2.11 s	MgO
1.27 vs	2.52 m	2.01 s	Al_3Ni_2 or NiAl
1.20 w*	2.45 s		
1.08 vs	2.27 w	1.49 s	MgO
	2.11 vs	1.42 s	Al_3Ni_2 or NiAl
	1.75 m	1.23 w	MgO
	1.68 vvw		
Solid rings	1.64 vw	Dotted rings (trace)	
	1.49 vs		
2.76 vw	1.40 vw	2.05 vvw	Ni_3Al
2.41 vw	1.35 w	1.78 vw	Ni_3Al
1.98 vw	1.32 vvw	1.26 s	Ni_3Al
1.40 vs	1.22 m	1.07 m	Ni_3Al
	0.94 s	0.81 m	Ni_3Al

Further RTA at 1000 °C for 100 s yields the patterns and microstructures shown in Fig. 5, and listed in Table III. The MgO/Al/Ni film exhibits a number of clear semi-solid rings which match lines seen at 800 °C. It is tempting to attribute these to the same phases (i.e. NiAl and MgO), in which case the conclusion is that the two are compatible even at 1000 °C. On the other hand, all lines match quite well a spinel phase, either $NiAl_2O_4$ (JCPDS 10-339) or $MgAl_2O_4$. There is also extensive nickel agglomeration in the form of "globules" of material with diameters in the 0.2–1 μm range, in both MgO/Al/Ni and Al/Ni films. These globules also appear in Al_2O_3/Al/Ni and ZrO_2/Al/Ni but not in SiC/Al/Ni films [7], and are similar to the nickel globules in Ni/C reactions [4]. The nickel segregation implies that NiAl has broken up, freeing nickel. The presence of a spinel and free nickel points to a reaction such as

$$2NiAl + 4MgO \rightarrow NiAl_2O_4 + Ni + 4Mg \quad (1)$$

or

$$2NiAl + 4MgO \rightarrow MgAl_2O_4 + 2Ni + 3Mg \quad (2)$$

The molecular ratio of MgO/NiAl, taking a total of 60 nm MgO and the thicknesses of the individual

TABLE III Interplanar spacings of the films in Table II, further annealed at 1000 °C for 100 s. Same notations as in Table II

Ni/Al	MgO	MgO/Al/Ni
Solid ring	Dotted rings	Semi-solid rings
1.40 vs	5.11 m	4.68 w
	4.33 vw	2.88 m
	3.90 s	2.44 s
	3.73 m	2.02 s
	3.49 s	1.66 vw
		1.55 m
	3.02 m	1.43 s
	2.79 s	
	2.52 s	Dotted rings (trace)
	2.48 m	
	2.27 m	5.12 w
	2.17 s	3.92 m
	2.03 vw	3.49 m
	1.95 vw	2.78 m
	1.89 vw	2.52 m
	1.75 vs	2.32 m
		2.18 w

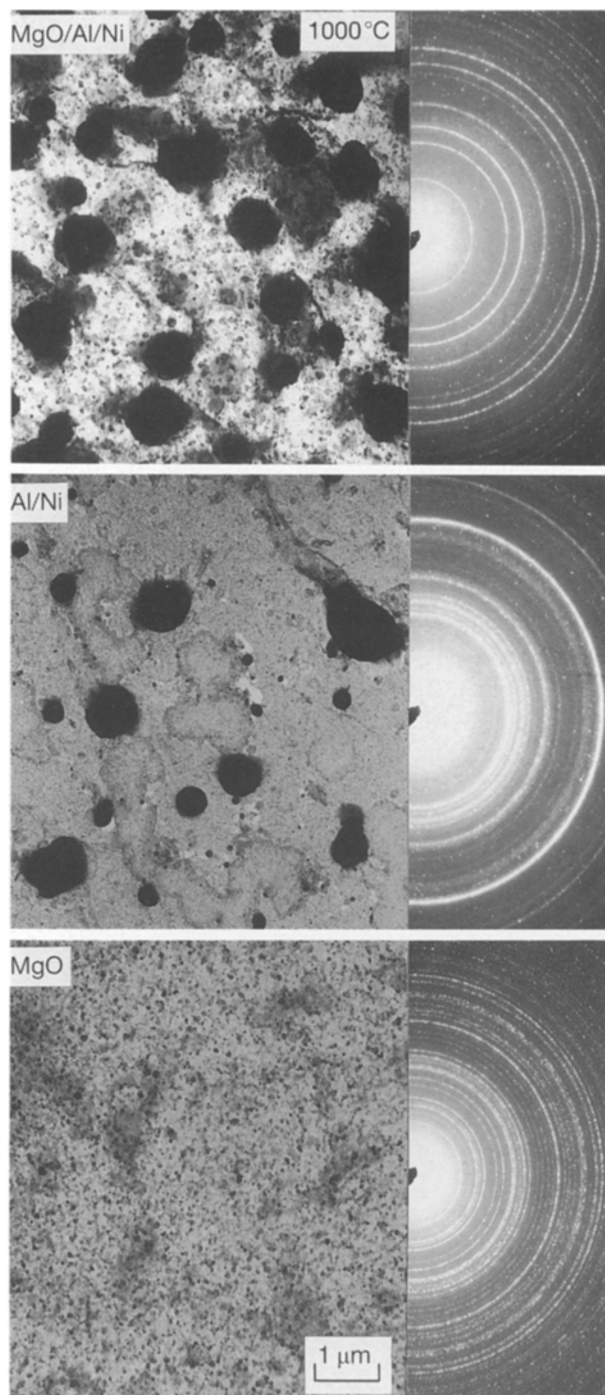

Figure 5 SAD patterns of films after additional annealing at 1000 °C for 100 s.

constituents of NiAl, is roughly 1.77 [3]. Given uncertainties in phase identification and in layer thicknesses, the above reactions can be reasonably considered balanced. Reaction 2 explains better the large amount of material in the nickel globules, and requires less free magnesium to "disappear" from the film. The MgO film exhibits an excellent polycrystalline pattern which, however, does not match any standard magnesium oxide file. The identity of this $Mg(O_x)$ phase remains a mystery; it could be a new magnesium-deficient, high-temperature MgO phase, possibly induced by the evaporation of magnesium from the film. The small-grained phase also appears in a MgO/Al/Ni film annealed separately only at 1000 °C for 100 s. Its similar texture in the two films is an indication that the changes in the MgO are partially independent of the presence of the aluminide.

The Al/Ni film is completely oxidized, with an extremely strong (4 4 0) γ-Al_2O_3 line plus minor amounts of unidentified phases (one of which may well be $NiAl_2O_4$, because a few lines seem to overlap the main lines in the MgO/Al/Ni film). The absence of the (4 4 0) γ-Al_2O_3 line in MgO/Al/Ni films means that NiAl oxidation due to residual oxygen in the annealing chamber is a much slower process than the MgO/NiAl interfacial reaction. In other words, artefacts introduced by oxygen diffusion through the MgO film to the MgO/NiAl interface do not affect our results significantly.

3.2. XPS

XPS depth profiles are useful mainly at lower temperatures, where the interaction of MgO with the SiO_2/Si substrate is limited. Profiles of a 300 °C annealed film, and the same film after 800 and 1000 °C annealings, are shown in Fig. 6. After 300 °C, Fig. 6a, one sees clearly the MgO/"NiAl"/MgO sandwich on top of the SiO_2 layer. The bottom (closer to SiO_2) MgO/Al interface is very sharp, while the top one is much broader, due to partial aluminium oxidation during the evaporation of MgO. The apparent nickel segregation to the sides of the Al/Ni multilayer structure is puzzling, and may be due in part to some artefact of the sputtering process, as well as due to the aluminium oxidation at the top interface. Note, however, that the average Al/Ni layer stoichiometry is indeed close to equiatomic. The MgO stoichiometry, calculated after calibrations with MgO crystals, is also close to the expected 1:1.

After exposure at 800 °C, an interfacial reaction between MgO and NiAl is clearly visible. Limiting ourselves to the top interface in order to avoid artefacts introduced by the MgO/SiO_2 reaction, we see the formation of a wide Mg–O–Al region which, in accord with the SAD data, is probably composed of the spinel $MgAl_2O_4$. The top MgO layer is still largely intact, but contains about 10% Al, which has diffused out of the aluminide. The out-diffusion of nickel is negligible, in marked contrast with the findings of Bobeth *et al.* [8], who identified nickel as the major diffusant out of Ni_3Al in an early oxidation stage. We submit that this contradiction is due to the different aluminide stoichiometry, and possibly due to the different microstructures. It seems clear, though, that with increased aluminium content and with polycrystalline aluminide, aluminium and not the noble component will, in fact, be the first major diffusing species at the aluminide–oxide interface, as seen also in $TiAl/Al_2O_3$ reactions [2], and in other studies [9]. This has obvious implications for the choice of a diffusion barrier, which, if required, should target aluminium and not the noble component. It is also worthwhile noting that oxygen diffusion into the aluminide occurs concurrently, as it did in $TiAl/Al_2O_3$ reactions [2].

The XPS profile of the 1000 °C annealed film, Fig. 6c, is not very instructive due to the extensive

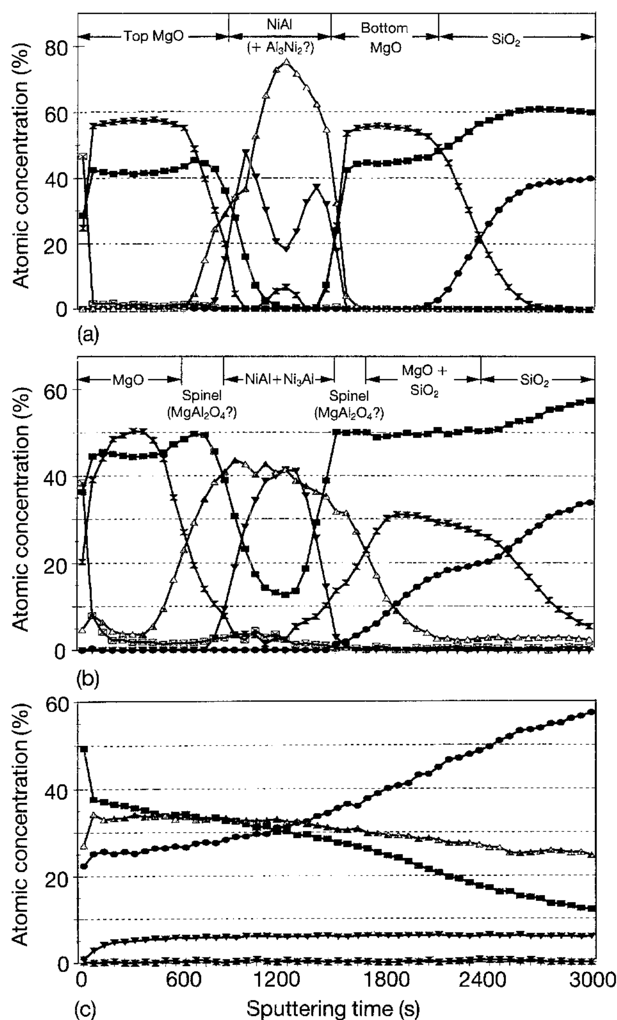

Figure 6 XPS depth profiles of films on oxidised Si substrates; a) after 300 °C annealing; b) after additional 800 °C annealing; c) after additional 1000 °C annealing. The atom percentages have errors on the order of 5–10% due to uncertain sensitivity factors and overlapping peaks. Symbols: ▼-Ni, △-Al, X-Mg, ■-O, ●-Si, ☒-C.

film–substrate reaction, which complicates tremendously the interpretation. This artefact can be eliminated, of course, by using MgO as a substrate, an experiment which is in progress. Nevertheless, some aspects of the MgO/NiAl reaction are clear: first, magnesium has disappeared from the film, and this is not due to its diffusion into the substrate. Thus, the issue raised by Misra regarding magnesium evaporation in a dynamic environment is confirmed. Second, the constant, low concentration of nickel, can best be explained by its existence in the form of globules distributed throughout the film, because once the distinct layer structure has broken up, phases coexisting side-by-side would give rise to a "smeared-out" depth profile. A direct comparison with the TEM results is, of course, impossible, but a certain conclusion is that the approximately 50 nm thick aluminide layer has disintegrated.

4. Conclusion

The initial stages of the NiAl/MgO interfacial reaction has been investigated; NiAl was found to react with MgO at predicted operation temperatures. Even taking into consideration the possible differences between thin polycrystalline film and bulk reactivities, it is still likely that a limited interfacial reaction will occur in bulk composites, following roughly the same steps, and leading to the formation of a spinel and Ni_3Al. A limited nanoscale interfacial reaction, as pointed out, is not necessarily detrimental, as it may lead to strong bonding and therefore good mechanical strength. On a *relative* basis, when compared with other systems such as $NiAl/ZrO_2$, $NiAl/Y_2O_3$, NiAl/SiC, $TiAl/Al_2O_3$ and TiAl/MgO, investigated by the same method [2, 7], the MgO/NiAl reaction at 800 °C is more limited, indicating that it is indeed one of the more stable aluminide-based IMCs.

Acknowledgements

This work was performed under ONR contract N00014-91-C-0168, monitored by Dr S. Fishman. We thank Mr Gil Mendenilla for his technical assistance.

References

1. A. K. MISRA, NASA Contractor Report 4171 (1988).
2. M. NATHAN, C. R. ANDERSON and J. S. AHEARN, *Mater. Sci. Eng.* **A162** (1993) 107.
3. M. NATHAN and J. S. AHEARN, *J. Mater. Sci. Lett.* in press.
4. *Idem, J. Appl. Phys.* **70** (1991) 811.
5. Joint Committee on Powder Diffraction Standards, "Powder Diffraction File" (International Center for Diffraction Data, Swarthmore, PA, 1985).
6. J. DOYCHAK, J. L. SMIALEK and T. E. MITCHELL, *Met. Trans.* **20A** (1989) 499.
7. M. NATHAN, unpublished.
8. M. BOBETH, W. POMPE, E. SCHUMANN and M. RUHLE, *Acta Metall. Mater.* **40** (1992) 2669.
9. J. DOYCHAK, J. A. NESBITT, R. D. NOEBE and R. R. BOWMAN, *Oxid. Metals* **38** (1992) 45.

Received 16 September 1993
and accepted 28 April 1994